IEEE Access
Multidisciplinary | Rapid Review | Open Access Journal

Received December 15, 2020, accepted December 27, 2020, date of publication January 11, 2021,
date of current version January 12, 2021.

Digital Object Identifier 10.1109/ACCESS.2020.3048927

Wideband Microwave Absorber Comprising Metallic Split-Ring Resonators Surrounded With E-Shaped Fractal Metamaterial

R. M. H. BILAL[1], M. A. BAQIR[2], P. K. CHOUDHURY[3], (Senior Member, IEEE), M. KARAASLAN[4], M. M. ALI[5], O. ALTINTAS[4], A. A. RAHIM[1], E. UNAL[4], AND C. SABAH[6]

[1]Faculty of Electrical Engineering, Ghulam Ishaq Khan Institute of Engineering Sciences and Technology, Topi 23100, Pakistan
[2]Department of Electrical and Computer Engineering, COMSATS University Islamabad, Sahiwal 57000, Pakistan
[3]Institute of Microengineering and Nanoelectronics, Universiti Kebangsaan Malaysia (UKM), Bangi 43600, Malaysia
[4]Department of Electrical and Electronics Engineering, Iskenderun Technical University, 31200 Iskenderun, Turkey
[5]Centre for Precision Engineering, Materials and Manufacturing Research, Institute of Technology, Sligo, F91 YW50 Ireland
[6]Department of Electrical and Electronics Engineering, Middle East Technical University at Northern Cyprus, 99738 Kalkanli, Turkey

Corresponding author: P. K. Choudhury (pankaj@ukm.edu.my)

This work was supported in part by the Higher Education Commission (HEC), Pakistan, under Grant 21-1811/SRGP/R&D/HEC/2017, and in part by the Universiti Kebangsaan Malaysia, Malaysia under Grant GP-2019-K018239.

ABSTRACT A specially designed metallic E-shaped fractal-based perfect metamaterial absorber (PMA) with fairly wideband absorptivity in the K- and Ka-bands of the microwave regime was investigated. The PMA top surface is comprised of square-shaped split-ring resonators (SRRs) surrounded with the stated fractal design. The absorptivity of PMA was analyzed in the range of 20−30 GHz for the normal and oblique incidence of waves. Both the transverse electric (TE) and transverse magnetic (TM) modes were taken up to observe the robustness of the proposed design. It was observed that the fractal resonators exhibit capacitive effect at low frequencies, whereas the SRRs manifest capacitive effect at higher frequencies. The simulation and measured results were found to be in fairly good agreement. It is expected that the proposed design of PMA would be useful for 5G communication applications.

INDEX TERMS Metamaterial, metamaterial absorber, fractal metasurface, fractal designs.

I. INTRODUCTION

Metamaterials (MMs) are the artificially engineered mediums, wherein periodically repeated subwavelength-sized metallic or dielectric unit cells are arranged to exhibit unique and exotic electromagnetic (EM) properties [1]–[4]. These find potentials in optical imaging [5], cloaking mediums [6], antennas [7], holography [8], ultra-sensitive sensors [9]–[12], filters [13], [14], perfect absorbers [15]–[18], etc. [19]–[21].

As known well, perfect absorption remains one of the interesting applications of MMs. Within the context, perfect metamaterial absorbers (PMAs) have been investigated with narrow and wideband absorption characteristics, depending on the application [15], [22]–[24]. Apart from these, the usages of PMA in wireless communication, emitters, sensors, photodetectors, photovoltaic solar cells and infrared camouflages are some of the notable ones [25]–[29].

To date, several forms of PMAs have been reported for suitably operating in the microwave, terahertz, visible and ultraviolet regimes [13], [30]–[32]. The desired absorption band can be essentially achieved by tailoring/optimizing the geometric parameters of the constituent meta-atoms (or the unit cells). Also, such *three-layer* PMAs work on the phenomenon of resonance, that include the top metasurface allowing penetration by the incidence EM waves, the middle substrate traps the radiation, and the bottom layer blocks the transmission of the same.

In the context of absorbers, different techniques have been exploited by the researchers to broaden the bandwidth employing multi-resonators in a super unit cell and/or multilayer structures [24], [29]. However, the drawbacks, such as large size, fabrication complexities, and high cost, very often suffice. Some other techniques exploit the use of

The associate editor coordinating the review of this manuscript and approving it for publication was Muguang Wang.

slot-loading [33], frequency selective surfaces [34] and fractals [21], [32], [35]. It remains rather challenging to achieve broadband absorption with the use of a single metasurface layer in designing PMAs.

Interestingly, the absorption band can be significantly enhanced by exploiting the concept of fractals – the repeated elements arranged in a specific pattern – in the metasurface architecture. Fractals possess the features, such as self-similarity, space-filling, and scaling. By carefully designing and selecting the shape of unit cell, thereby contributing to construct the proposed device, wideband and miniaturized microwave and optical devices can be implemented. The present work relies on the fractal space-filling property that contributes to miniaturization and the self-similarity, and creates multiple resonances to attain wideband features [35]–[37].

In this investigation, we aim at developing a fractal metamaterial absorber (FMA) comprising metallic SRRs surrounded by E-shaped fractals. We analyse the absorption spectrum of the resulting metasurface-based design in the 20–30 GHz microwave regime, for both the TE- and TM-incidence excitations. We also consider the effects of incidence obliquity and substrate thickness to observe relatively wideband absorption – the feature that indicates the proposed structure to have potentials for application in the K- and Ka-bands. The results indicate the use of FMA in 5G communication as well as MIMO (massive-input and massive output) antennas.

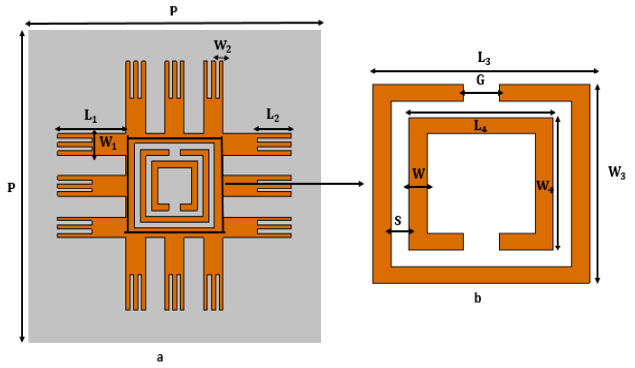

FIGURE 1. Schematic of the proposed fractal metamaterial absorber; (a) top view, and (b) enlarged view of metallic split-ring geometry at the center.

II. DESIGN AND MODELING

Figure 1a shows the unit cell of the top metasurface architecture of the proposed FMA, whereas fig. 1b exhibits the central SRR design used as a component of the unit cell. The FMA itself is a metal-dielectric-metal kind of three-layer configuration, wherein the top and bottom layers are composed of copper (having the conductivity $\sigma = 5.8\times10^7$ S/m) separated by the FR_4 dielectric material (having the relative permittivity $\varepsilon_r = 4.3$ and loss tangent $\tan\delta = 0.025$). As becomes clear from fig. 1a, the meta-atom has metallic E-shaped fractal-like structure with the inclusion of two square-shaped asymmetric metallic SRRs at the center.

While optimizing the metasurface design, we start with the edge-to-edge connected four equidimensional square copper patches, each having a size of 8.5×8.5 mm^2. We then convert each of these patches to assume symmetric E-shaped design of the first-order fractal kind. Similarly, the next fractal stages can be achieved from the previous ones without disturbing the symmetry of each E-shaped structure. In the final step, two asymmetric square-shaped SRRs are inserted at the central void space of the edge-to-edge connected fractals. Finally, following the symbols in fig. 1, we use the design parameters as $P = 26$ mm, $L_1 = 6$ mm, $W_1 = 1.7$ mm, $L_2 = 3$ mm, $W_2 = 0.34$ mm, $L_3 = W_3 = 6$ mm, $L_4 = W_4 = 4$ mm, $W = S = 0.5$ mm, and $G = 1$ mm. Also, we consider the thickness of metasurface to be 32 μm. Using the proposed metasurface, the FMA 3D configuration assumes the form, as depicted in fig. 2.

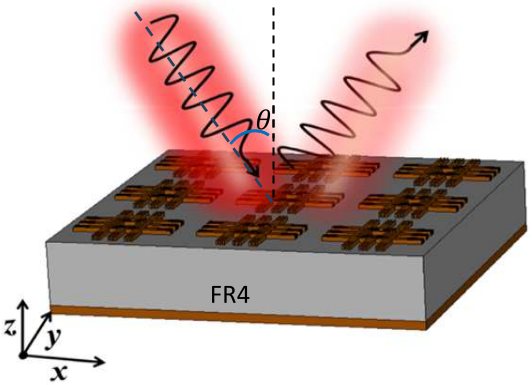

FIGURE 2. Schematic of the proposed FMA configuration.

We first use the CST Microwave Studio simulation, in order to investigate the absorption characteristics of the proposed FMA structure. In such an attempt, we employ the unit cell boundary conditions along the x- and y-directions, while the open add space boundary conditions along the z-direction. Further, a time-harmonic plane wave is excited along the z-direction. Upon illuminating the top fractal metasurface, the overall absorption is determined as [35].

$$A(\omega) = 1 - T(\omega) - R(\omega) \tag{1}$$

$$A(\omega) = 1 - |S_{21}(\omega)|^2 - |S_{11}(\omega)|^2 \tag{2}$$

where

$$|S_{11}(\omega)|^2 = \left|S_{11_{xx}}(\omega)\right|^2 + \left|S_{11_{yx}}(\omega)\right|^2 \tag{3}$$

Here the subscripts 'xx' and 'yx' correspond to the co- and cross-components, respectively. In our proposed design, the cross-reflection component is almost vanishing, i.e., $\left|S_{11_{yx}}(\omega)\right| = 0$, thereby giving rise to

$$A(\omega) = 1 - \left|S_{11_{xx}}(\omega)\right|^2 \tag{4}$$

It is noteworthy that the bottom ground plane of the FMA (fig. 2) behaves as a perfect reflector to block the transmission of waves, and therefore, the transmission coefficient $S_{21} \sim 0$, thereby making the absorption features to be controlled by the reflection characteristics only. To achieve perfect absorption, the magnitude of reflection should be almost vanishing – the feature that can be achieved by attaining suitable resonance conditions. Interestingly, at resonance, the effective impedance of the top fractal metasurface (of the absorber) matches with the free-space impedance, which essentially would result into the absorption of entire incidence radiation (by the PMA structure). The normalized impedance Z of metamaterial is defined as $Z = (1 + S_{11}) / (1 - S_{11})$ [38].

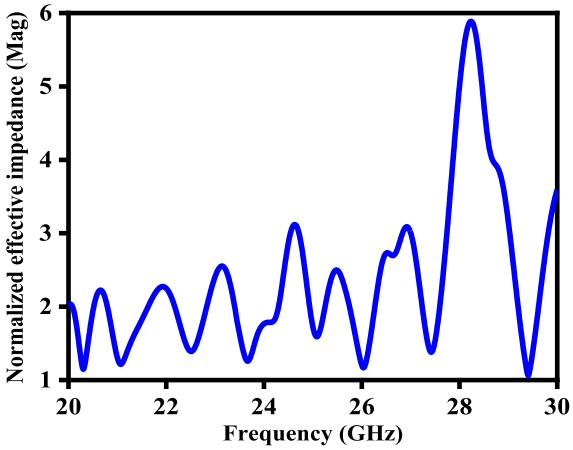

FIGURE 3. Effective impedance of the proposed FMA.

Figure 3 shows the frequency-dependence of the normalized effective impedance of the proposed top metasurface. According to the impedance matching condition (i.e., $Z = 1$), the EM waves would penetrate metasurface. We observe in fig. 2 that the impedance pattern exhibits ripples. However, it becomes unity at 29.5 GHz frequency – the value at which the incidence waves will pass through the metasurface with vanishing reflection. Apart from this, the impedance exhibits values close to unity corresponding to some other frequencies as well, namely 20.4 GHz, 21 GHz, 23.7 GHz and 26 GHz.

III. RESULTS AND DISCUSSION

As stated in Section 2, in order to optimize the wideband absorption property of the proposed FMA, we start with designing and simulating different fractal stages of the unit cell considering the normal incidence of EM radiation. Figure 4 exhibits the frequency dependence of absorptivity, considering the four different stages of fractal geometry, taking into account the transverse electric (TE) and transverse magnetic (TM) incidence polarizations.

In this stream, we first take the zeroth-order fractal stage; fig. 4a illustrates the obtained absorption characteristics and the fractal design in the inset (of figure). We observe the presence of multiple absorption peaks at different frequencies.

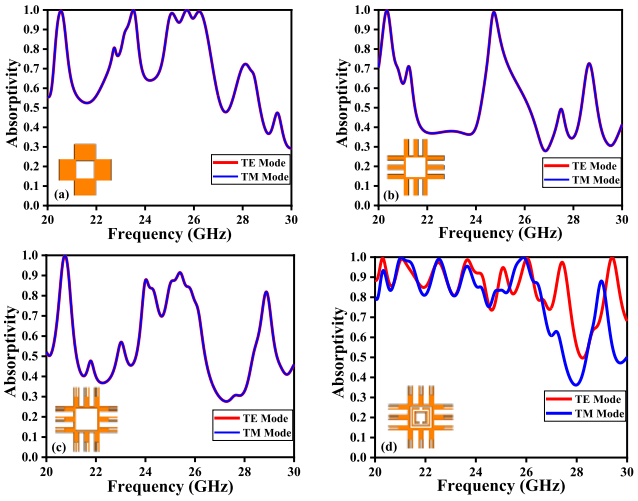

FIGURE 4. Frequency dependence of absorptivity of the proposed FMA considering (a) zero-order, (b) first-order, and (c) second-order fractals, and (d) second-order fractal with SRRs; all under normal incidence.

We find the absorption patterns corresponding to the TE- and TM-polarized excitations overlap, thereby making the FMA to be polarization-insensitive – the feature that is attributed to the four-fold symmetry of the unit cell in the metasurface. Upon using the first-order fractal structure in the unit cell design, which we achieve by converting each square patch into the form of E-shaped resonator (the inset of fig. 4b), we still obtain the polarization-insensitive multi-band absorption patterns (fig. 4b). The spectral characteristics are, however, significantly altered now, as compared to what we observe in fig. 4a. The second-order fractal geometry (as in the inset of fig. 4c) in the metasurface unit cell also exhibits the polarization-insensitive behavior, as fig. 4c shows. In all these three cases, we observe very high (polarization-insensitive) absorption in the frequency range of 20–21 GHz. Interestingly, the impedance characteristic in fig. 3 also shows nearly unity value of impedance, thereby confirming high absorption of incidence radiation. Corresponding to some other frequency values as well, for which the impedance values are close to unity (fig. 3), we obtain high absorptivity in figs. 4a–c.

Next, we attempt to insert two asymmetric metallic SRRs into the central void space of the second-order E-shaped fractal geometry; the inset of fig. 4d exhibits the unit-cell structure used in the metasurface. We clearly observe in this case that the polarization-insensitive property of metasurface is lifted off as the absorption spectra corresponding to the TE- and TM-polarized incidence radiations are distinct now. This is essentially attributed to the incorporation of asymmetric SRRs in the metasurface. In fact, the four-fold symmetry in the unit cell structure is lost in this case due to the inclusion of two asymmetric split-rings, thereby eliminating the polarization-insensitive characteristics of the FMA. Further, though the absorption patterns exhibit ripples, the overall absorptivity remains broader in frequency range in this case. Apart from this, we obtain very high

absorption corresponding to several impedance values which remains close to unity (in fig. 3); the increase in absorptivity is attributed to the capacitive effect of the two asymmetric split-rings.

A deeper insight into fig. 4d gives the minimum absorption of over 80% in the frequency range of 20–24 GHz. Within this span, the FMA exhibits even perfect absorption corresponding to certain values of frequency, namely 20.4 GHz, 21 GHz, 22.5 GHz, and 23.7 GHz. Outside the range of 20–24 GHz, the FMA yields perfect absorption at 29.5 GHz as well. Interestingly, corresponding to all these frequency values, fig. 3 exhibits the impedance to be either unity or close to unity.

We discussed above the results considering the normal incidence (i.e., $\theta = 0°$) of the TE- and TM-polarized excitations. We now investigate the absorption characteristics of FMA under the oblique incidence of EM waves. For this purpose, we vary the obliquity angle in a range of 0°–40° in a step of 10°. Also, we take two different values of substrate thickness, viz. 1.2 mm and 1.6 mm; figs. 5 and 6, respectively, illustrate the achieved frequency-dependent absorption characteristics.

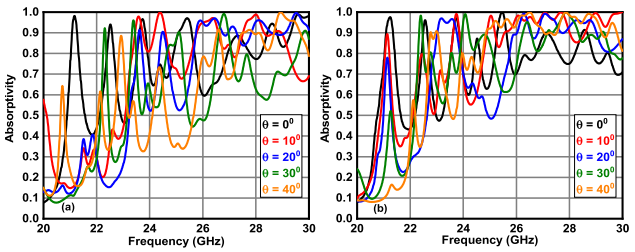

FIGURE 5. Frequency-dependent absorptivity of the proposed FMA under different obliquities considering the (a) TE-, and (b) TM-polarized incidence excitations, and the dielectric layer thickness as 1.2 mm.

Figure 5 illustrates the obtained spectral patterns; figs. 5a and 5b, respectively, being corresponding to the TE- and TM-polarized incidence conditions. We observe in these figures that all the used values of incidence obliquity show ripples in the absorption spectra in the used range of operating frequencies. However, the proposed FMA exhibits nearly perfect absorption as well corresponding to certain frequency values. In the context of observing multiband absorption in the frequency range of 20–30 GHz, we notice in fig. 5a that, for the normal incidence (i.e., $\theta = 0°$; fig. 2) of TE-polarized waves, multiband absorption peaks are located at the operating frequencies ∼21.06 GHz, 22.2 GHz, 23.36 GHz, 24.9 GHz, 27.9 GHz, and 29 GHz with the respective absorptivity values as ∼98.31%, 94.24%, 96.76%, 97.11%, 94.71% and 96%. The increase of obliquity to 10° yields the peak absorption values to be ∼97.75%, 99.99%, 97.11% and 99%, and positioned at the respective operating frequencies as ∼23.6 GHz, 24.3 GHz, 26.4 GHz, and 28 GHz. The use of $\theta = 20°$ gives ∼91.59% and 91% absorptions at 23.5 GHz and 24.3 GHz frequencies, respectively, and a wideband absorptivity of ∼85% in the 25.5–30 GHz span. Further increase of obliquity values to 30° and 40° also results in multiple absorption peaks. Overall, fig. 5a reveals that the increase of incidence angle of the TE-polarized wave generally results in lowering the absorptivity.

The absorption spectra corresponding to the TM-polarized incidence excitation (fig. 5b) show almost similar trend of resulting in multiple absorption peaks, as observed in the case of impinging TE-polarized waves (fig. 5a). The positions of absorption peaks and the respective magnitudes of absorption can be observed from these figures, which indicate that the absorptivity is generally larger for higher frequencies, and its values typically become lower with the increase in obliquity. This is essentially attributed to the resonance conditions, which alter upon changing the incidence angle [39], [40]. Furthermore, the absorption band is also reduced with increasing obliquity (fig. 5).

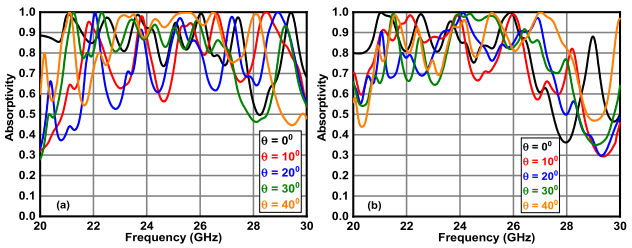

FIGURE 6. Frequency-dependent absorptivity of the proposed FMA under different obliquities considering the (a) TE-, and (b) TM-polarized incidence excitations, and the dielectric layer thickness as 1.6 mm.

Now, as stated before, fig. 6 corresponds to the absorption patterns with increased value of dielectric medium thickness, i.e., 1.6 mm. We observe in this figure that the spectral characteristics are almost similar to what fig. 5 depicts (when the FR4 medium thickness is 1.2 mm) except for some minor alterations only. As such, a small increase in the FR4 layer thickness would not leave significant impact on the absorption features of this FMA.

In order to give a comparative look at the present work considering some of the previously reported results in similar context [39]–[45], we incorporate Table 1 to emphasize the importance of this investigation. In most of these earlier works, wideband absorption was attained by exploiting multilayered configurations in designing the absorber. Reference [41] reports the largest absorption band, which could be achieved exploiting the metamaterial absorber comprised of polymer and carbon nanotubes. The design essentially involves a multilayer kind of structure, which somehow remains relatively costly to fabricate. Apart from this, the use of multilayer structures somehow imposes limitations on practical applications in the modern communication technology where systems generally require miniaturized devices. Table 1 determines the proposed kind of FMA to be attractive in achieving fairly wideband characteristic.

We now plot the electric field and surface current distributions corresponding to two different absorption peaks, as obtained under the normal incidence of TE-polarized

TABLE 1. Comparison of the present work with some of the previously reported works.

Reference numbers	Operating frequency	Materials used	Configuration	Absorption bandwidth (> 80%)	Remarks
[39]	2–24 GHz	FR4 and copper	Multilayer	12–22 GHz	Large thickness and costly fabrication
[40]	8–16 GHz	FR4 and copper	Multilayer	Multiband	Bandwidth limitation
[41]	5–40 GHz	Polymer and carbon nanotube	Multilayer	8–40 GHz	Costly fabrication
[42]	2–20 GHz	FR4 and copper	Multilayer	5–19 GHz	Large thickness and costly fabrication
[30]	6–15 GHz	FR4 and copper	Multilayer	7.8–14.7 GHz	Large thickness and costly fabrication
[43]	1–30 GHz	FR4 and copper	Multilayer	4.52–25.42 GHz	Costly fabrication
[44]	5–25 GHz	FR4, Teflon and copper	Multilayer	7.5–21 GHz	Costly fabrication
[45]	3–25 GHz	Rogers TMM4, teflon and copper	Multilayer	8–21.5 GHz	Large thickness and costly fabrication
Proposed work	20–30 GHz	FR4 and copper	Single layer	20–28 GHz	Easy fabrication

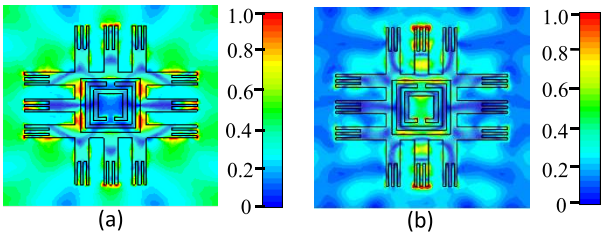

FIGURE 7. Electric field distribution patterns of FMA at (a) 21 GHz, and (b) 29 GHz.

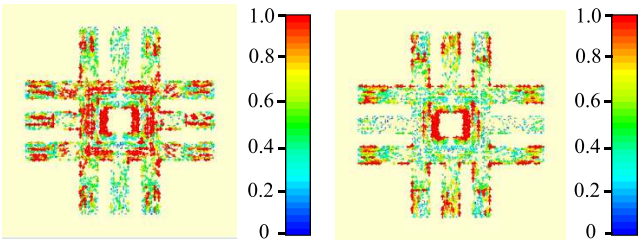

FIGURE 8. Surface current distribution patterns of FMA at (a) 21 GHz, and (b) 29 GHz.

wave; figs. 7 and 8 exhibit these. In particular, figs. 7a and 7b, respectively, depict the electric field intensity patterns at the top metasurface of FMA corresponding to the absorption peaks at 21 GHz and 29 GHz, whereas figs. 8a and 8b exhibit the respective surface current distributions at these frequency values. We notice in fig. 7a that the electric field is maximally localized at the edges of metallic E-shaped resonators, whereas fig. 7b shows its maximum concentration at the center of the used SRRs as well as in the middle legs of the E-shaped resonators located at the upper and lower ends of split-rings. These support the wavelength-dependent absorption of the proposed metamaterial structures. In fig. 8, the current is maximally distributed in the SRRs at the center.

In order to experimentally verify the results, we attempt to fabricate the proposed FMA structure. For this purpose, we prepare the sample consisting of 6×6-unit cells of copper medium, fabricated over the FR4 dielectric substrate with a thickness of 1.6 mm, as fig. 9 illustrates. The fabrication process has been realized by using the CNC-based LPKF E33 prototyping machine equipped with the plotting and milling techniques.

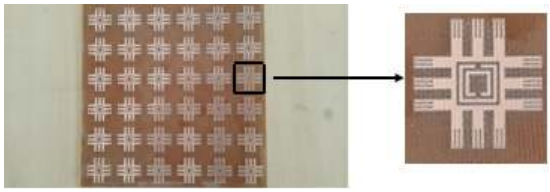

FIGURE 9. Fabricated sample of the FMA comprised of 6 × 6-unit cells (left) and the unit cell itself (right).

The experimental setup for reflection measurement has been achieved by using the Agilent PNA-L Vector Network Analyzer (VNA) having an operating frequency band in the range of 10 MHz to 43.5 GHz. We use horn antennas with an operating frequency span of 15–40 GHz, in order to measure the absorptivity of the proposed structure at normal incidence of radiation having frequencies 20–30 GHz. We fix the distance between horn antennas and the FMA sample by considering the far-field region approximation, according to

which the field can be assumed to be simply as normal (to the FMA surface) EM radiation. As such, we take the far-field distance to be $\gg 2D^2/\lambda$ with D being the highest antenna dimension and λ is the center wavelength.

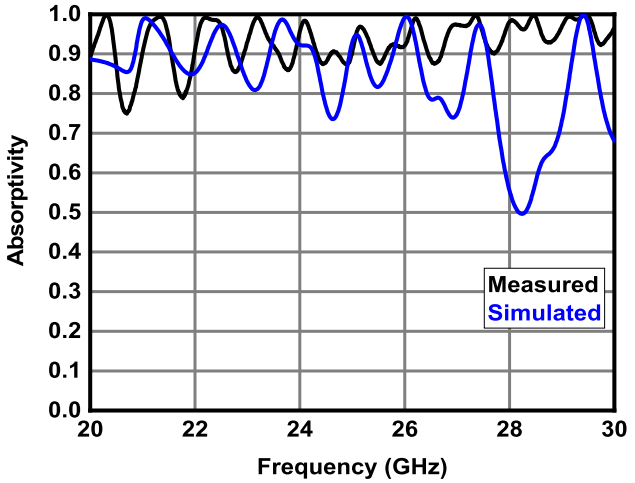

FIGURE 10. Simulated and measured frequency-dependent absorptivity of the proposed FMA.

Before proceeding for measurements, we first calibrate the VNA by using a special calibration kit having a short-circuit, open-circuit and load connectors. After that, we place antennas at the front side of FMA, and measure the reflected power (S_{11}) – the parameter that we use to extract the value of absorption. Figure 10 exhibits the measured and simulated results together, which determine the frequency-dependent absorptivity of the proposed FMA structure. Also, we observe both the results to be in good agreement at certain frequencies in the used operating frequency span. Overall, the results may be considered to be in fairly good agreement in the 20–27.5 GHz frequency range. However, there remains significant mismatch between the 28 GHz and 29 GHz frequency points, which may be attributed to calibration errors and/or minor disturbances around. Minor deviations from the ''perfect-fabrication'' of FMA would also cause such discrepancies. Disturbances in the measured absorptivity pattern would also arise due to imperfect laboratory conditions and test cables. Calibration errors for such high-frequency applications would also introduce instabilities in the absorptivity plots. Nonetheless, the measurement and simulation results show that the proposed FMA structure has an average of ∼80% absorption in the frequency range of 20–30 GHz.

IV. CONCLUSION

In the afore discussed results, we investigated the absorption characteristics of a new type of metallic E-shaped fractal-based FMA structure, which incorporates asymmetric square-shaped metallic SRRs at the center, in the 20−30 GHz (i.e., for the K and Ka-bands) frequency span exploiting the simulation and experimental routes, and find the obtained results to be in fairly good agreement. The simulation results corresponding to different orders of fractal design indicate the use of SRRs at the center of fractal geometry lifts up the polarization-insensitive property of the resulting metasurface. However, the use of fractal metasurface without exploiting the asymmetric SRRs at the center allows the FMA to remain polarization-insensitive, which is owing to the four-fold symmetry in the fractal geometry. Also, minor changes in the dielectric substrate thickness do not leave major impact on the absorption spectra. In average, the FMA attains the largest absorptivity of ∼80% for the normal incidence of waves with the TE- and TM-polarized excitations. At certain operating frequencies, however, the structure also exhibits nearly perfect absorption of waves. The proposed absorber covers the 5G frequency band, and therefore, it would be useful for the future 5G communication systems for filtering, antenna isolation, and attenuation related applications.

ACKNOWLEDGMENT

The authors acknowledge fruitful comments by the anonymous reviewers, which helped improving the text.

REFERENCES

[1] D. R. Smith, S. Schultz, P. Markoš, and C. M. Soukoulis, ''Determination of effective permittivity and permeability of metamaterials from reflection and transmission coefficients,'' *Phys. Rev. B, Condens. Matter*, vol. 65, no. 19, Apr. 2002, Art. no. 195104.

[2] Z. Y. Duan, C. Guo, and M. Chen, ''Enhanced reversed Cherenkov radiation in a waveguide with double-negative metamaterials,'' *Opt. Exp.*, vol. 19, no. 15, pp. 13825–13830, Jul. 2011.

[3] C. Sabah, F. Dincer, M. Karaaslan, O. Akgol, E. Demirel, and E. Unal, ''New-generation chiral metamaterials based on rectangular split ring resonators with small and constant chirality over a certain frequency band,'' *IEEE Trans. Antennas Propag.*, vol. 62, no. 11, pp. 5745–5751, Nov. 2014.

[4] Z. Duan, X. Tang, Z. Wang, Y. Zhang, X. Chen, M. Chen, and Y. Gong, ''Observation of the reversed Cherenkov radiation,'' *Nature Commun.*, vol. 8, no. 1, p. 14901, Apr. 2017.

[5] N. Fang, H. Lee, C. Sun, and X. Zhang, ''Sub–diffraction-limited optical imaging with a silver superlens,'' *Science*, vol. 308, no. 5721, pp. 534–537, 2005.

[6] D. Schurig, J. J. Mock, B. J. Justice, S. A. Cummer, J. B. Pendry, A. F. Starr, and D. R. Smith, ''Metamaterial electromagnetic cloak at microwave frequencies,'' *Science*, vol. 314, no. 5801, pp. 977–980, 2006.

[7] T. Liu, X. Cao, J. Gao, Q. Zheng, W. Li, and H. Yang, ''RCS reduction of waveguide slot antenna with metamaterial absorber,'' *IEEE Trans. Antennas Propag.*, vol. 61, no. 3, pp. 1479–1484, Mar. 2013.

[8] L. Huang, S. Zhang, and T. Zentgraf, ''Metasurface holography: From fundamentals to applications,'' *Nanophotonics*, vol. 7, no. 6, pp. 1169–1190, Jun. 2018.

[9] O. Altınta , M. Aksoy, and E. Ünal, ''Design of a metamaterial inspired omega shaped resonator based sensor for industrial implementations,'' *Phys. E, Low-Dimensional Syst. Nanostruct.*, vol. 116, Feb. 2020, Art. no. 113734.

[10] K. V. Sreekanth, P. Mahalakshmi, S. Han, M. S. M. Rajan, P. K. Choudhury, and R. Singh, ''Brewster mode-enhanced sensing with hyperbolic metamaterial,'' *Adv. Opt. Mater.*, vol. 7, no. 21, Nov. 2019, Art. no. 1900680.

[11] M. A. Baqir and P. K. Choudhury, ''On the VO_2 metasurface-based temperature sensor,'' *J. Opt. Soc. Amer. B, Opt. Phys.*, vol. 36, no. 8, pp. F123–F130, 2019.

[12] M. Ghasemi, N. Roostaei, F. Sohrabi, S. M. Hamidi, and P. K. Choudhury, ''Biosensing application of all-dielectric SiO_2-PDMS meta-stadium grating nanocombs,'' *Opt. Mater. Exp.*, vol. 10, no. 4, pp. 1018–1033, 2020.

[13] Y. Yang, Y. Xu, B. Zhang, J. Duan, L. Yan, H. Xu, Y. Liu, and Y. Shi, ''Investigating flexible band-stop metamaterial filter over THz,'' *Opt. Commun.*, vol. 438, pp. 39–45, May 2019.

[14] M. Pourmand and P. K. Choudhury, ''Wideband THz filtering by graphene-over-dielectric periodic structures with and without MgF_2 defect layer,'' *IEEE Access*, vol. 8, pp. 137385–137394, 2020.

[15] J. Zhu, Z. Ma, W. Sun, F. Ding, Q. He, L. Zhou, and Y. Ma, "Ultra-broadband terahertz metamaterial absorber," *Appl. Phys. Lett.*, vol. 105, no. 2, Jul. 2014, Art. no. 021102.
[16] M. A. Baqir and P. K. Choudhury, "Hyperbolic metamaterial-based UV absorber," *IEEE Photon. Technol. Lett.*, vol. 29, no. 18, pp. 1548–1551, Sep. 15, 2017.
[17] M. A. Baqir and P. K. Choudhury, "Design of hyperbolic metamaterial-based absorber comprised of ti nanospheres," *IEEE Photon. Technol. Lett.*, vol. 31, no. 10, pp. 735–738, May 15, 2019.
[18] R. M. H. Bilal, M. A. Baqir, P. K. Choudhury, M. A. Naveed, M. M. Ali, and A. A. Rahim, "Ultrathin broadband metasurface-based absorber comprised of tungsten nanowires," *Results Phys.*, vol. 19, Dec. 2020, Art. no. 103471.
[19] H. Chen, J. Wang, H. Ma, S. Qu, Z. Xu, A. Zhang, M. Yan, and Y. Li, "Ultra-wideband polarization conversion metasurfaces based on multiple plasmon resonances," *J. Appl. Phys.*, vol. 115, no. 15, Apr. 2014, Art. no. 154504.
[20] M. A. Baqir, P. K. Choudhury, A. Farmani, T. Younas, J. Arshad, A. Mir, and S. Karimi, "Tunable plasmon induced transparency in graphene and hyperbolic metamaterial-based structure," *IEEE Photon. J.*, vol. 11, no. 4, pp. 1–10, Aug. 2019.
[21] R. M. H. Bilal, M. A. Baqir, P. K. Choudhury, M. M. Ali, and A. A. Rahim, "Tunable and multiple plasmon-induced transparency in a metasurface comprised of silver S-shaped resonator and rectangular strip," *IEEE Photon. J.*, vol. 12, no. 3, pp. 1–13, Jun. 2020.
[22] T. Nesimoglu and C. Sabah, "A tunable metamaterial resonator using varactor diodes to facilitate the design of reconfigurable microwave circuits," *IEEE Trans. Circuits Syst. II, Exp. Briefs*, vol. 63, no. 1, pp. 89–93, Jan. 2016.
[23] S. Liu, H. Chen, and T. J. Cui, "A broadband terahertz absorber using multi-layer stacked bars," *Appl. Phys. Lett.*, vol. 106, no. 15, Apr. 2015, Art. no. 151601.
[24] S. Kang, Z. Qian, V. Rajaram, S. D. Calisgan, A. Alù, and M. Rinaldi, "Ultra-narrowband metamaterial absorbers for high spectral resolution infrared spectroscopy," *Adv. Opt. Mater.*, vol. 7, no. 2, Jan. 2019, Art. no. 1801236.
[25] Y. Wang, T. Sun, T. Paudel, Y. Zhang, Z. Ren, and K. Kempa, "Metamaterial-plasmonic absorber structure for high efficiency amorphous silicon solar cells," *Nano Lett.*, vol. 12, no. 1, pp. 440–445, Jan. 2012.
[26] M. Kenney, J. Grant, Y. D. Shah, I. Escorcia-Carranza, M. Humphreys, and D. R. S. Cumming, "Octave-spanning broadband absorption of terahertz light using metasurface fractal-cross absorbers," *ACS Photon.*, vol. 4, no. 10, pp. 2604–2612, Oct. 2017.
[27] Y. Wu, J. Wang, S. Lai, X. Zhu, and W. Gu, "Transparent and flexible broadband absorber for the sub-6G band of 5G mobile communication," *Opt. Mater. Exp.*, vol. 8, no. 11, pp. 3351–3358, 2018.
[28] J. Li, C. Zhao, B. Liu, C. You, F. Chu, N. Tian, Y. Chen, S. Li, B. An, A. Cui, X. Zhang, H. Yan, D. Liu, and Y. Zhang, "Metamaterial grating-integrated graphene photodetector with broadband high responsivity," *Appl. Surf. Sci.*, vol. 473, pp. 633–640, Apr. 2019.
[29] N. Lee, T. Kim, J.-S. Lim, I. Chang, and H. H. Cho, "Metamaterial-selective emitter for maximizing infrared camouflage performance with energy dissipation," *ACS Appl. Mater. Interfaces*, vol. 11, no. 23, pp. 21250–21257, Jun. 2019.
[30] F. Ding, Y. Cui, X. Ge, Y. Jin, and S. He, "Ultra-broadband microwave metamaterial absorber," *Appl. Phys. Lett.*, vol. 100, no. 10, Mar. 2012, Art. no. 103506.
[31] J. Huang, J. Li, Y. Yang, J. Li, J. Li, Y. Zhang, and J. Yao, "Broadband terahertz absorber with a flexible, reconfigurable performance based on hybrid-patterned vanadium dioxide metasurfaces," *Opt. Exp.*, vol. 28, no. 12, pp. 17832–17840, 2020.
[32] R. M. H. Bilal, M. A. Saeed, P. K. Choudhury, M. A. Baqir, W. Kamal, M. M. Ali, and A. A. Rahim, "Elliptical metallic rings-shaped fractal metamaterial absorber in the visible regime," *Sci. Rep.*, vol. 10, no. 1, p. 14035, Dec. 2020.
[33] T. T. Nguyen and S. Lim, "Design of metamaterial absorber using eight-resistive-arm cell for simultaneous broadband and wide-incidence-angle absorption," *Sci. Rep.*, vol. 8, no. 1, p. 6633, Dec. 2018.
[34] F. Costa and A. Monorchio, "A frequency selective radome with wideband absorbing properties," *IEEE Trans. Antennas Propag.*, vol. 60, no. 6, pp. 2740–2747, Jun. 2012.
[35] T. Chen, S.-J. Li, X.-Y. Cao, J. Gao, and Z.-X. Guo, "Ultra-wideband and polarization-insensitive fractal perfect metamaterial absorber based on a three-dimensional fractal tree microstructure with multi-modes," *Appl. Phys. A, Solids Surf.*, vol. 125, no. 4, p. 232, Apr. 2019.
[36] S. J. Li, Y. B. Li, H. Li, Z. X. Wang, C. Zhang, Z. X. Guo, R. Q. Li, X. Y. Cao, Q. Cheng, and T. J. Cui, "A thin self-feeding Janus metasurface for manipulating incident waves and emitting radiation waves simultaneously," *Annalen der Physik*, vol. 532, no. 5, May 2020, Art. no. 2000020.
[37] S. J. Li, T. J. Cui, Y. B. Li, C. Zhang, R. Q. Li, X. Y. Cao, and Z. X. Guo, "Multifunctional and multiband fractal metasurface based on inter-metamolecular coupling interaction," *Adv. Theory Simul.*, vol. 2, no. 8, 2019, Art. no. 1900105.
[38] D. R. Smith, D. C. Vier, T. Koschny, and C. M. Soukoulis, "Electromagnetic parameter retrieval from inhomogeneous metamaterials," *Phys. Rev. E, Stat. Phys. Plasmas Fluids Relat. Interdiscip. Top.*, vol. 71, no. 3, Mar. 2005, Art. no. 036617.
[39] M. R. Soheilifar and R. A. Sadeghzadeh, "Design, fabrication and characterization of stacked layers planar broadband metamaterial absorber at microwave frequency," *AEU-Int. J. Electron. Commun.*, vol. 69, no. 1, pp. 126–132, Jan. 2015.
[40] D.-E. Wen, X. Huang, L. Guo, H. Yang, S. Han, and J. Zhang, "Quadruple-band polarization-insensitive wide-angle metamaterial absorber based on multi-layer structure," *Optik*, vol. 126, nos. 9–10, pp. 1018–1020, May 2015.
[41] Y. Danlée, I. Huynen, and C. Bailly, "Thin smart multilayer microwave absorber based on hybrid structure of polymer and carbon nanotubes," *Appl. Phys. Lett.*, vol. 100, no. 21, May 2012, Art. no. 213105.
[42] S. Ghosh, S. Bhattacharyya, and K. V. Srivastava, "Design, characterisation and fabrication of a broadband polarisation-insensitive multi-layer circuit analogue absorber," *IET Microw., Antennas Propag.*, vol. 10, no. 8, pp. 850–855, Jun. 2016.
[43] S.-J. Li, P.-X. Wu, H.-X. Xu, Y.-L. Zhou, X.-Y. Cao, J.-F. Han, C. Zhang, H.-H. Yang, and Z. Zhang, "Ultra-wideband and polarization-insensitive perfect absorber using multilayer metamaterials, lumped resistors, and strong coupling effects," *Nanosc. Res. Lett.*, vol. 13, no. 1, p. 386, Dec. 2018.
[44] L. L. Cong, X. Y. Cao, T. Song, J. Gao, and J. X. Lan, "Angular- and polarization-insensitive ultrathin double-layered metamaterial absorber for ultra-wideband application," *Sci. Rep.*, vol. 8, no. 1, p. 9627, Dec. 2018.
[45] H. Xiong, J.-S. Hong, C.-M. Luo, and L.-L. Zhong, "An ultrathin and broadband metamaterial absorber using multi-layer structures," *J. Appl. Phys.*, vol. 114, no. 6, Aug. 2013, Art. no. 064109.

R. M. H. BILAL received the B.S. degree in electronic engineering from the Islamia University of Bahawalpur, Pakistan, in 2014, and the M.S. degree in electronic engineering from the Ghulam Ishaq Khan Institute (GIK) of Engineering Sciences and Technology, Topi, Pakistan, in 2018. He was a Graduate Research Assistant with the Faculty of Electrical Engineering, GIK Institute, from 2016 to 2018. He is currently affiliated with the Lahore University of Management Sciences, Lahore, Pakistan. He has authored or coauthored six journal articles in his research interests. His research interests include electromagnetics, antennas, metamaterials and optics. He is a member of Pakistan Engineering Council (PEC), Pakistan.

M. A. BAQIR received the M.Sc. and M.Phil. degrees in electronics from the Department of Electronics, Quaid-i-Azam University, Pakistan, in 2008 and 2011, respectively, and the Ph.D. degree from the Institute of Microengineering and Nanoelectronics, Universiti Kebangsaan Malaysia, Malaysia, in 2017. Since 2017, he has been an Assistant Professor with the Department of Electrical and Computer Engineering, COMSATS University Islamabad, Pakistan. He has earned more than 45 publications in reputed peer-reviewed international journals and conference proceedings, and a book chapter. His current research interests include light-matter interactions, photonic crystals, 2D materials, periodic structures, core-shell nanoparticles, and absorbers. He serves as a reviewer for several journals, including IEEE Antenna and Wireless Propagation Letters, *Journal of Electromagnetic Waves and Applications*, IEEE Photonics Journal, IEEE Sensors Journal, *IET Micro and Nano Letters*, and *IET Power Electronics*.

P. K. CHOUDHURY (Senior Member, IEEE) received the Ph.D. degree in physics, in 1992. He held academic positions in India, Canada, Japan, and Malaysia. From 2003 to 2009, he was a Professor with the Faculty of Engineering, Multimedia University, Cyberjaya, Malaysia. He joined professorship at the Institute of Microengineering and Nanoelectronics, Universiti Kebangsaan Malaysia, Malaysia. He also served as the Telekom Research and Development (TMR&D), Malaysia, as a Consultant, for a couple of projects on optical devices. He has published over 250 research articles, contributed chapters to 17 books, and edited and co-edited six research level books. His research interests include the theory of optical waveguides, which include complex mediums, fiber optic devices, optical sensors, and metamaterial properties. He is a Senior Member of OSA and SPIE. He is a reviewer for over three dozen research journals. He is also the Section Editor of *Optik*—International Journal for Light and Electron Optics (Elsevier, The Netherlands) and the Editor-in-Chief of the *Journal of Electromagnetic Waves and Applications* (Taylor & Francis, U.K.).

M. KARAASLAN received the Ph.D. degree in physics from the University of Cukurova, Adana, Turkey, in 2009. He is the coauthor of about 130 scientific contributions published in journals and conference proceedings. His research interests include the applications of metamaterials, analysis and synthesis of antennas, and waveguides.

M. M. ALI received the B.S. degree in electronics engineering from the Islamia University of Bahawalpur, Pakistan, in 2009, the M.S. degree in electronics engineering from the Ghulam Ishaq Khan Institute (GIK) of Engineering Sciences and Technology, Topi, Pakistan, in 2012, and the Ph.D. degree in photonic engineering from the University of Malaya, Kuala Lumpur, Malaysia, in 2016. From 2017 to 2018, he was an Assistant Professor with the Faculty of Electrical Engineering, GIK Institute, and from 2018 to 2020, he was a Postdoctoral Researcher with the Department of Electronic and Computer Engineering, University of Limerick, Ireland. He is currently a Postdoctoral Researcher with the Centre for Precision Engineering, Materials and Manufacturing Research, Institute of Technology Sligo, Ireland. His research interests include photonics and communications, microwave engineering, advanced digital signal and image processing, and laser welding of polymers. He is a member of the Pakistan Engineering Council and the National Academy of Young Scientists, Pakistan. He is a Fellow of the Pakistan Academy of Engineers. He is also a Guest Editor of the Special Issue on Optical Fibre Based Pressure and Temperature Sensors for Biomedical and Industrial Applications of IEEE Sensors Journal.

O. ALTİNTAS received the B.Sc. degree in electrical and electronics engineering from Cukurova University, Adana, Turkey, in 2011, the M.Sc. degree from Mustafa Kemal University, Hatay, Turkey, in 2015, and the Ph.D. degree in electrical and electronics engineering from Cukurova University, in 2020. He worked on microwave metamaterial-based sensors for industrial implementations. He has authored or coauthored 30 scientific contributions published in technical journals. His research interests include microwave sensors, absorbers, energy harvesters, and polarization converters in the microwave regime.

A. A. RAHIM received the B.S. degree in electrical engineering from the University of Engineering and Technology (UET), Peshawar, Pakistan, in 2008, the M.S. degree from the GIK Institute, Pakistan, in 2011, and the Ph.D. degree in electrical engineering from the Politecnico di Torino, Italy, in 2015. Since July 2015, he has been working as an Assistant Professor with the Faculty of Electrical Engineering, GIK Institute. His research interests primarily include computational micromagnetics, magnonics, metamaterials and metasurfaces, optics, and photonics. He has authored/coauthored numerous publications in his research fields.

E. UNAL received the Ph.D. degree in electrical and electronics engineering from the University of Gaziantep, Turkey, in 1994. He has coauthored about 50 scientific contributions published in international books, journals, and peer-reviewed conference proceedings. His research interests include frequency selective surfaces and metamaterials.

C. SABAH received the B.Sc., M.Sc., and Ph.D. degrees in electrical and electronics engineering. He is currently a Professor with the Electrical and Electronics Engineering Department, Middle East Technical University (Northern Cyprus Campus), where he is also a Secretary General and an Advisor to the President. His research interests include the microwave and electromagnetic investigation of unconventional materials and structures, wave propagation, scattering, complex media, metamaterials and their applications, and solar systems.